INTERNATIONAL JOURNAL
FOR RESEARCH

IN APPLIED SCIENCE & ENGINEERING TECHNOLOGY

Satellite-Based Spatiotemporal Evaluation of Urban Growth Impacts on Surface Energy Balance and Thermal Conditions in Mumbai, India

Mahi Patel[1], Ajay Patel[2], Hetkumar Parmar[3]

[1]Ph.D. Scholar, Silver Oak Institute of Science, Silver Oak University, Ahmedabad, India – 382481
[2]Student of M.Tech, CEPT University, Ahmedabad, India - 380009
[3]Student of MCA, A.M. Patel Institute of Computer Studies, Ganpat University, Mehsana, India – 384012

Abstract: This study examines the spatiotemporal variations in land use/land cover (LULC), land surface temperature (LST), and surface energy fluxes in Mumbai, India, from 2014 to 2024 using Landsat 8 (OLI/TIRS) data and the SEBAL (Surface Energy Balance Algorithm for Land) model on the Google Earth Engine (GEE) platform. Built-up areas expanded from 18.6% to 30.5%, while natural vegetation declined from 37.8% to 27.7%, indicating rapid urban growth and ecological stress. LST increased by about 2 °C, showing a strong inverse relationship with the Normalized Difference Vegetation Index (NDVI), emphasizing the role of vegetation loss in urban heat amplification. Surface energy balance results revealed a 34.9% increase in net radiation (Rn) and higher sensible heat flux (H) in dense urban zones, while latent heat flux (LE) and evapotranspiration (ET) remained low and vegetation-dependent. Seasonal patterns highlighted elevated Rn and H during summer, with LE peaking in the monsoon. Correlation analysis confirmed a strong positive link between ET and LE ($R^2 = 1.0$) and a negative correlation with H ($R^2 = 0.44$). Findings suggest that urbanization intensifies thermal stress and alters energy dynamics, stressing the need for vegetation-based climate adaptation strategies in city planning.
Keywords: Thermal Conditions, Urban growth Impact, Surface Energy Balance, Land Use Change, Remote Sensing,

I. INTRODUCTION

The development in terms of urban sprawl at the expense of natural land cover has also become a major cause of climate variability both locally and regionally. Urbanization has a significant impact on affecting the surface energy balance (SEB) due to changes in land cover, surface roughness, albedo, emissivity, and moisture availability. The alterations of such changes disturb the natural process of splitting the incoming solar radiation into the net radiation (Rn), sensible heat flux (H), latent heat flux (LE) and ground heat flux (G) thus worsening the power of beholding urban heat island (UHI) intensity and abridging the resiliency of the urban climate (Sultana & Satyanarayana, 2023). Nonetheless, along with the increasing attention to the role of the surface energy exchanges in urban microclimate formulation, the existing gap in high-resolution, seasonally specific, and geographically situated research is notable, especially in semi-arid Indian cities where vegetation and urban morphology changes enormously depending on the season (Bala et al., 2024).

Surface Energy Balance Algorithm for Land (SEBAL) and Surface Energy Balance System (SEBS), which have become one of the standard methods to estimate the SEB components with the help of satellite-based data like land surface temperature (LST), normalized difference vegetation index (NDVI), albedo, and emissivity (Sultana & Satyanarayana, 2021) (Saxena et al., 2024). However, several studies in which these models have been used were based on coarse spatial resolution data like MODIS or AVHRR (250–1000 m) of adequate data in terms of regional extent climate. When it comes to evaluating climate at the city scale, such approaches are often insufficient for capturing the intra-urban variability necessary for detailed spatial analysis (Eswar et al., 2017). Simplification of localized variation in surface energy fluxes yields a simplistic view of the urban thermal processes, in particular, in heterogeneous cities where the contrast between land cover and imperviousness tends to be strong and significant (Rahman & Zhang, 2019). Medium resolutions, such as Landsat 8, capable of at least 30 m spatial optical and 100 m spatial thermal and nearly a 100 percent increase in spatial extremes and variation in urban form resolution, pose tremendous benefits to the urban SEB research (Zawadzka et al., 2019)(Firozjaei et al., 2024). In addition, the development of cloud computing tools, including Google Earth Engine (GEE), to combine Landsat data and their availability has allowed researchers to analyze numerous and long-running data sets of geospatial information within a reasonable time (Liang et al., 2020).

International Journal for Research in Applied Science & Engineering Technology (IJRASET)
ISSN: 2321-9653; IC Value: 45.98; SJ Impact Factor: 7.538
Volume 14 Issue III Mar 2026- Available at www.ijraset.com

Nevertheless, limited studies have been done to utilize the full potential of Landsat 8 to estimate the total components of SEB (in a multi-year and multi-season urban setting) in an Indian environment (Barletta et al., 2022). Most existing studies have primarily addressed specific SEB components such as land surface temperature (LST) and evapotranspiration (ET), focusing on short-term periods that inadequately capture interannual variability and long-term urbanization effects (Taheri et al., 2022)(Ramírez-Cuesta et al., 2022).

Recent studies have examined surface energy balance (SEB) components in urban areas across India and Los Angeles. In Indian cities, sensible heat flux (SHF) increased while latent heat flux (LHF) slightly decreased from 2000-2018, with SHF showing a positive correlation to land surface temperature (Sultana & Satyanarayana, 2021). Urban areas and bare soil exhibited higher ground heat flux ratios compared to vegetated areas, while vegetation and water bodies showed higher LHF ratios (Bala et al., 2022). In a semi-arid region of the Deccan Plateau, SHF dominated over LHF even during the monsoon season, with soil moisture and net radiation playing crucial roles in surface flux partitioning (Anand et al., 2022). In Los Angeles, latent heat fluxes displayed spatial and temporal responses to irrigation and regional climate, with peak latent heat occurring 3 hours before solar noon due to early morning irrigation practices (Wetherley et al., 2021). Comparative studies between cities with distinct climates but similar summer conditions reveal that vegetation fraction is inversely related to Bowen ratios, while impervious surfaces correlate positively with sensible heat partitioning (Estoque et al., 2017). These findings highlight the importance of considering both spatial and climatic contexts when designing urban areas to mitigate urbanization effects on local climate.

The study addresses research gaps by conducting a decade-long (2014–2024) spatiotemporal analysis of the urban surface energy balance in Mumbai, using Landsat 8 satellite images and the SEBAL model within the Google Earth Engine (GEE) platform. It utilized variables obtained from satellite data, such as land surface temperature (LST), NDVI, albedo, and emissivity, to estimate main surface energy balance (SEB) parameters such as net radiation (Rn), sensible heat flux (H), latent heat flux (LE), and ground heat flux (G) with seasonal resolution of summer and monsoon seasons. The research examines the variability in spatial-temporal fluxes and evaluates the effect of seasonal land-use change, which contributes to a better understanding of urban energy dynamics in data-scarce environments. A study investigates the effects of urban development and vegetation coverage on the spatial pattern as well as the temporal aspects of surface energy fluxes. The results help understand urban thermal dynamics and contribute to the creation of climate-resilient strategies of urban planning.

II. MATERIALS & METHODS

Mumbai, the financial capital of India, is one of the most densely populated metropolitan regions in the western part of the country, situated between latitudes 18°53′00″N and 19°16′00″N and longitudes 72°47′00″E and 72°59′00″E, covering about 603 square kilometres (Rahaman et al., 2021). Mumbai functions as India's commercial, financial, and industrial hub, with a highly heterogeneous land use pattern that includes high-density residential areas, central business districts, industrial zones, transport corridors, slums, and fragmented green spaces.

Coastal and reclaimed regions display compact urban morphology with limited vegetation, intensifying Urban Heat Island (UHI) effects and elevated Land Surface Temperature (LST). In contrast, northern and eastern suburban areas preserve open spaces, mangroves, and vegetation patches that help moderate local microclimates. The city experiences a tropical climate with hot, humid summers (30–35 °C) from March to May, and heavy monsoon rains (June–September) accounting for over 90% of annual precipitation. Post-monsoon and winter months (October–February) are relatively mild (18–25 °C) (Rahaman et al., 2021). Urban development is overseen by the Municipal Corporation of Greater Mumbai (MCGM), the Mumbai Metropolitan Region Development Authority (MMRDA), and allied bodies.

Landsat 8 satellite imagery was employed to estimate Land Surface Temperature (LST), generate vegetation indices, and analyze surface energy flux parameters. Data spanning the period from 2014 to 2023 were processed using the Google Earth Engine (GEE) platform (Muhaimin et al., 2024).

The analysis utilized the Landsat 8 Collection-2 Tier-1 dataset (LANDSAT/LC08/C02/T1_L2), which provides Brightness Temperature (BT) and Top-of-Atmosphere (TOA) reflectance values. Landsat 8 carries two primary sensors: the Operational Land Imager (OLI) and the Thermal Infrared Sensor (TIRS) (USGS, 2024).
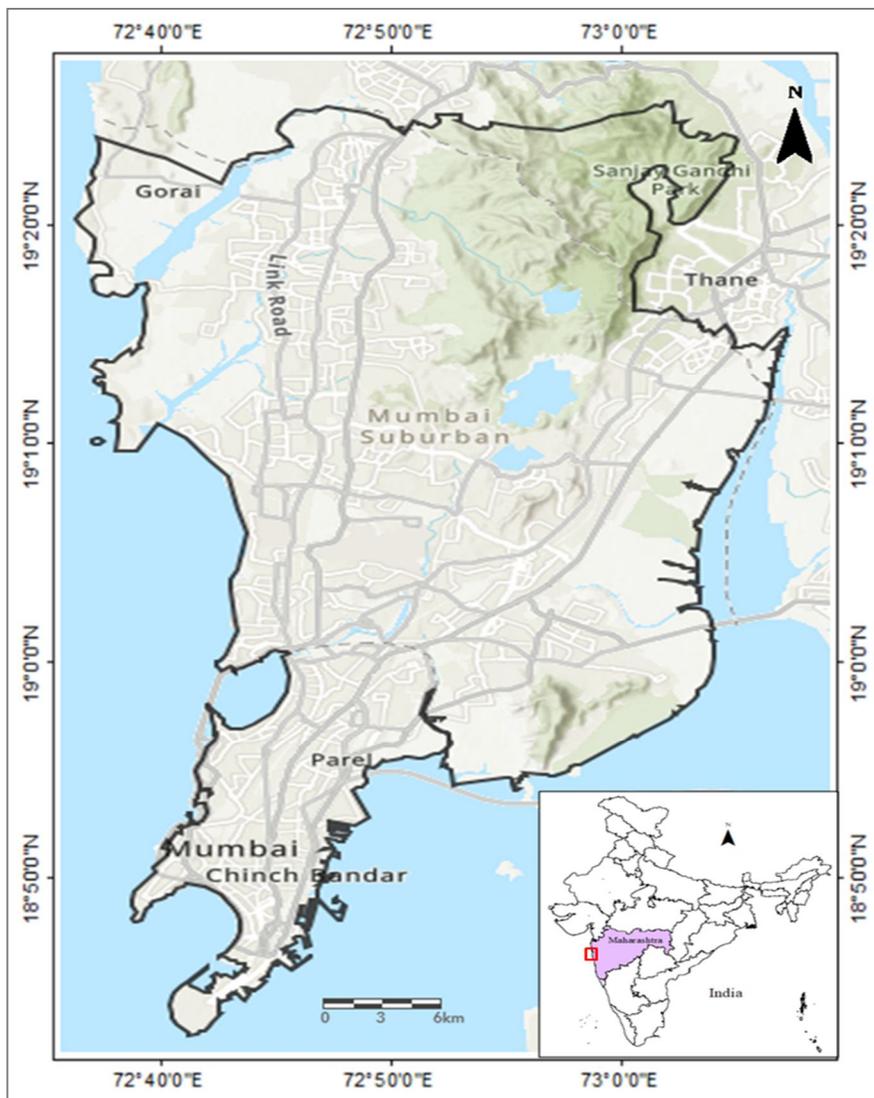
Figure 1. Study area

The OLI captures multispectral, non-thermal imagery at a spatial resolution of 30 meters (Table 1), primarily used for mapping land surface features. In contrast, TIRS collects thermal infrared data at a spatial resolution of 100 meters, which is essential for deriving LST (Govil et al., 2019).

Table 1. Dataset used in this Study

Dataset	Landsat-8 (OLI / TIR)
Data Collection from GEE	LANDSAT/LC08/C02/T1_L2
Resolution	OLI: 30 m (Band 2, 4, 5, 6, 7) TIR: 100 m (Band 10)
Band Information	B2: Blue $(0.45 – 0.51\mu m)$ B4: Red $(0.64 – 0.67\mu m)$ B5: NIR $(0.85 – 0.88\mu m)$ B5: SWIR1 $(1.57 – 1.65\mu m)$ B5: SWIR2 $(2.11 – 2.29\mu m)$ B10: TIR $(10.6 – 11.19\mu m)$

Figure 2 illustrates the comprehensive methodology flowchart developed for the estimation of Land Surface Temperature (LST), vegetation indices, albedo, surface energy flux components, and evapotranspiration over the urban and peri-urban regions of Mumbai for the period 2014–2023. The entire analysis was carried out using Google Earth Engine (GEE), a cloud-based geospatial analysis platform. Initially, Landsat 8 imagery was loaded and preprocessed, including cloud masking using the QA_PIXEL band to remove pixels flagged as clouds or cloud shadows through standard bitwise operations (Ermida et al., 2020). Radiometric and atmospheric corrections were applied using official Landsat scaling factors to ensure accurate surface reflectance values.
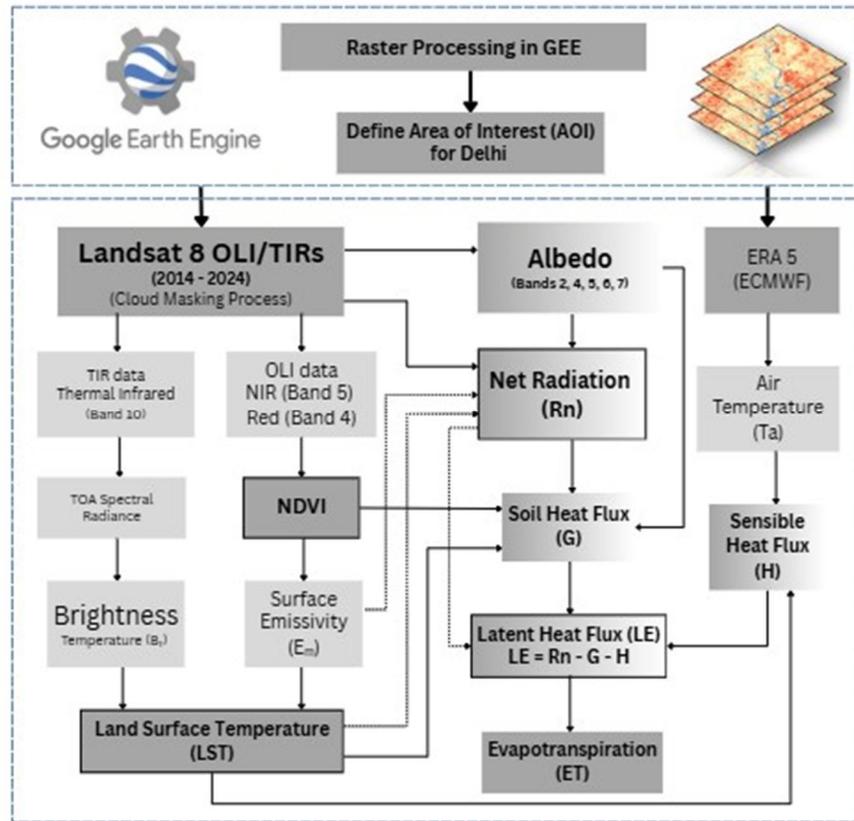

Figure 2. Flow chart of Methodology

The Brightness Temperature (B_T) is calculated using the thermal band of Landsat-8 as shown in equation (1) (Nikkala et al., 2022)

$$B_T = \left(\frac{K_2}{\ln\left(\frac{K_1}{L}+1\right)}\right) - 273.15 \quad \ldots\ldots\ldots\ldots\ldots(1)$$

Here, K_1 and K_2 are band-specific calibration constants in Kelvin, and B_T represents the effective satellite temperature, the K_1 and K_2 constants from the OLI/TIRS sensor (Shirani-bidabadi et al., 2019).

The Normalized Difference Vegetation Index (NDVI) is derived using the Red (Band 4) and Near-Infrared (NIR, Band 5) bands with equation (2) (Dissanayake et al., 2019).

$$NDVI = \frac{NIR-Red}{NIR+Red} \quad \ldots\ldots\ldots\ldots\ldots(2)$$

Land Surface Emissivity (LSE) is estimated using NDVI thresholds as per equation (3)

$Emissivity\ (E_m) = 0.004 \cdot Pv + 0.986 \ldots\ldots\ldots\ldots\ldots(3)$

The fraction of vegetation (P_v) is computed from NDVI values using equation (3a) (Simwanda et al., 2019)

$$P_v = \left(\frac{NDVI-NDVI_{min}}{NDVI_{max}-NDVI_{min}}\right)^2 \ldots\ldots\ldots\ldots\ldots(3a)$$

The Land Surface Temperature (LST) is calculated using B_T and E_m values in equation (4) (Sultana et al., 2020) (Patel et al., 2025)

$$LST = \frac{B_T}{1+\left(0.00115 \cdot \frac{B_T}{1.438} \ln(E_m)\right)} \quad \ldots\ldots\ldots\ldots\ldots(4)$$

Using equations (2) and (4), Annually mean values of NDVI and LST were calculated for the period from 2014 to 2023.

In addition the surface Albedo (α) is estimated using the reflectance values from the visible, near-infrared, and shortwave infrared bands of Landsat-8. It quantifies the ability of surface to reflect solar radiation (Barletta et al., 2022).

$$\alpha = 0.356 \cdot B_{Blue} + 0.130 \cdot B_{Red} + 0.373 \cdot B_{NIR} + 0.085 \cdot B_{SWIR1} + 0.072 \cdot B_{SWIR2} - 0.0018 \quad \dots\dots(5)$$

B_{Blue}, B_{Red}, B_{NIR}, B_{SWIR1}, and B_{SWIR2} are the surface reflectance values of Landsat 8 Bands 2, 4, 5, 6, and 7, respectively.

The incoming shortwave radiation ($R_s\downarrow$) was estimated using surface albedo and solar geometry parameters (solar zenith angle, earth-sun distance) extracted from the Landsat metadata (Ferreira et al., 2020). The outgoing longwave radiation ($R_l\uparrow$) was approximated using the Stefan–Boltzmann Law, assuming surface temperature as a proxy for atmospheric temperature:

$$R_l \uparrow = \varepsilon \cdot \sigma \cdot T_s^4 \quad \dots\dots\dots\dots\dots (6)$$

Where, ε is the surface emissivity; $\sigma = 5.67\times10{-8}$ W·m−2·K−4 is the Stefan–Boltzmann constant; T_s is the land surface temperature in Kelvin

Using the above inputs from equation (6) and (5), Net Radiation (R_n), which represents the total available energy at the surface, was calculated using the following energy balance equation (Silva et al., 2018):

$$R_n = (1 - \alpha) \cdot R_s \downarrow + \varepsilon \cdot R_l \downarrow - \varepsilon \cdot \sigma \cdot T_s^4 \quad \dots\dots\dots\dots\dots (7)$$

Where, α is the surface albedo; $R_s\downarrow$ is the incoming shortwave radiation; $R_l\downarrow$ is the incoming longwave radiation; $\varepsilon \cdot \sigma \cdot T_s^4$ represents the outgoing longwave radiation ($R_l\uparrow$).

The soil heat flux (G), which represents the conductive energy flux into the ground (Desai et al., 2022). This formulation integrates Rn, albedo and vegetation dynamics from equation (7), (5), (2) to modulate soil heat flux based on surface cover characteristics (Liang et al., 2022).

$$G = R_n \left((T_s - 273.15)(0.0038 + 0.0074 \cdot \alpha)(1 - 0.98 \cdot (NDVI)^4)\right) \quad \dots\dots\dots\dots\dots (8)$$

Where, R_n is the net radiation (W m^{-2}); T_s is the land surface temperature in Kelvin; α is the surface albedo; NDVI is the Normalized Difference Vegetation Index.

The sensible heat flux (H) is calculated based on the temperature gradient between the land surface and the near-surface air (Rios et al., 2022), using the following equation (Eq. 8):

$$H = \frac{\rho \cdot Cp \cdot (T_s - T_a)}{r_{ah}} \quad \dots\dots\dots\dots\dots (8)$$

Where, ρ is the air density (kg·m^{-3}); Cp is the specific heat of air at constant pressure (1005 J·kg^{-1}·K^{-1}); T_s is the land surface temperature (K); T_a is the near-surface air temperature (K); r_{ah} is the aerodynamic resistance to heat transport (s·m^{-1}).

The near-surface air temperature (T_a) (Jaiswal et al., 2023) was obtained from the ERA5-Land reanalysis dataset, provided by the European Centre for Medium-Range Weather Forecasts (ECMWF) and accessible via Google Earth Engine (GEE). This dataset offers hourly land-atmosphere variables at a spatial resolution of approximately 2 m. For the city of Mumbai, characterized by an urban landscape interspersed with vegetated areas, an aerodynamic resistance (r_{ah}) value of 60 s·m^{-1} was assumed.

The latent heat flux (LE), which indicates the amount of energy used for evapotranspiration, is obtained as the residual of the energy balance equation (Bala et al., 2024):

$$\boldsymbol{LE = R_n - G - H} \quad \dots\dots\dots\dots\dots (9)$$

Finally, the actual evapotranspiration (ET) in mm/day is derived using the latent heat flux (LE), and the latent heat of vaporization ($\lambda = 2.45 \times 10^6$ J/kg), as shown below (Silva et al., 2018):

$$ET = \frac{LE \cdot 86400}{\lambda} \quad \dots\dots\dots\dots\dots (10)$$

Where, 86400 is the number of seconds in a day. This approach enables pixel-wise ET estimation from satellite data across spatial and temporal domains.

In the final phase of the methodology, the impact of urbanization on vegetation cover and surface energy dynamics in Mumbai was assessed by analyzing long-term trends in NDVI, LST, and surface flux components. Using seasonal and annual raster datasets derived from Google Earth Engine, correlation analysis was performed to explore the interrelationship among variables (Patel et al., 2024). Specifically, the Pearson correlation coefficient was used to evaluate the linear associations between NDVI, LST, and net radiation (Rn), as well as between albedo and Rn, and LST and Rn. These relationships provide insights into how urban expansion influences surface energy balance and vegetation dynamics (Mohammad et al., 2019). Seasonal variation in surface fluxes was also analyzed, particularly comparing summer and monsoon periods, to understand the thermal and moisture redistribution under

changing land use (Rawal & Gupta, 2021). Furthermore, correlations between LE and H, and between LE and ET, were computed to assess how energy partitioning affects evapotranspiration processes in the urban landscape (Mathew et al., 2022). These analyses helped in identifying spatial and temporal patterns of land-atmosphere interactions under the pressure of urban growth and climatic variability.

III. RESULTS AND DISCUSSION

Analysis of surface energy flux components derived in Landsat 8 (OLI/TIR) imagery by the SEBAL model in the cloud-based Google Earth Engine (GEE) platform describes considerable annual tendencies in energy partitioning in the city of Mumbai between 2014-2024 as the effects of the vegetation dynamics and continuous urbanization in the city.

A. Land Use Change Detection

The evaluation of land use and land cover (LULC) dynamics across the decade of 2014-2024 in Mumbai indicates a sharp anthropogenic change in tune with that of urbanization witnessed in other semi-arid cities of India. As Figure (3) shows, there is a strong upward trend, with 18.6% of the built-up area in 2014 and 30.5% in 2024, which is a net increase of 11.9%. This pattern is consistent across the largest cities of India, where urban growth predominantly occurs through edge expansion, leading to the fragmentation of tree cover, agricultural lands, and water bodies (Agarwal et al., 2023). At the same time, the natural plants dropped sharply from 37.8% to 27.7%, showing that there was a lot of stress on the environment because of changes in land use, a finding also noted in the study by Vaishnav et al. (2024), which linked the loss of plants to higher water loss in growing urban areas. The reduction of barren land by 4.9% to 3.7% indicates the transformation of transitional surfaces into impervious structures. These trends show that the city is becoming more impervious and help to understand the origins of surface energy imbalance and the possible UHI effects. The proportion of water bodies fluctuated to 1% during the study period, maintaining the same consistency that may be attributed to the enhanced spatial resolution of Landsat 8 or localized systems like water retention systems. These interpretations were also proposed in the urban hydro studies of other municipalities in India (Agan et al., 2021). Therefore, the LULC modifications in Mumbai during the ten years reflect the generalized restructuring of the landscape brought on by urbanization in similar semi-arid regions. Which has serious implications for both the surface energy balance and environmental sustainability of the city and in composition constitutes one of the foundations for the perception of the land surface temperature and heat flux variations.
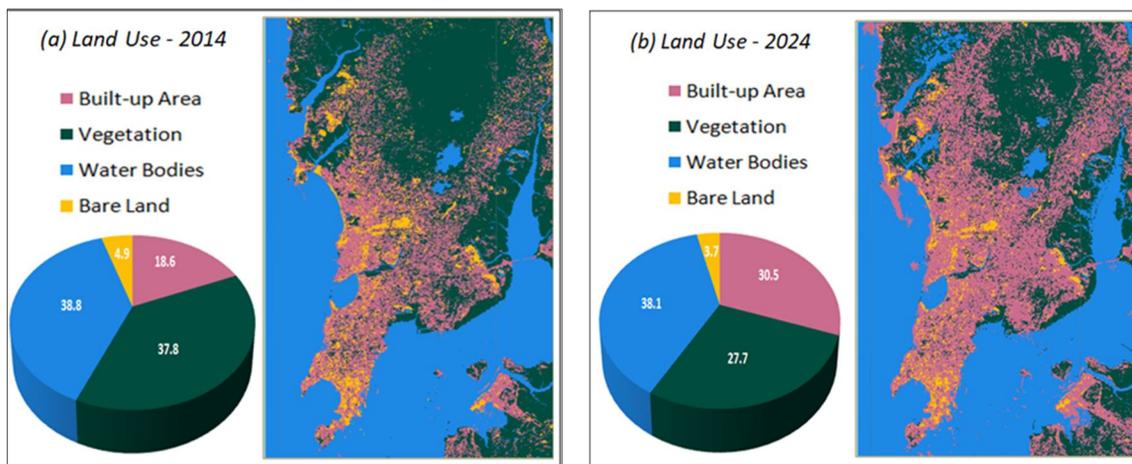

Figure 3. Land use classification for year (a) 2014 and (b) 2024

B. Temporal Analysis of LST and NDVI (2014–2024)

The increasing trend analysis of Land Surface Temperature (LST) and Normalized Difference Vegetation Index (NDVI) of Mumbai between 2014 and 2024 shows that there is a substantial negative correlation between LST and NDVI, which highlights the effect of rising temperature due to CO_2 emission in the context of diminishing vegetation cover, which is attributed to the urban sprawl. LST improved between 2014 (27.42°C) and 2024 (29.19°C) in a net increase of 2°C over ten years, as shown in Figure 4. The highest temperatures were recorded in 2022 (29.09°C), and 2017 (29.28°C).
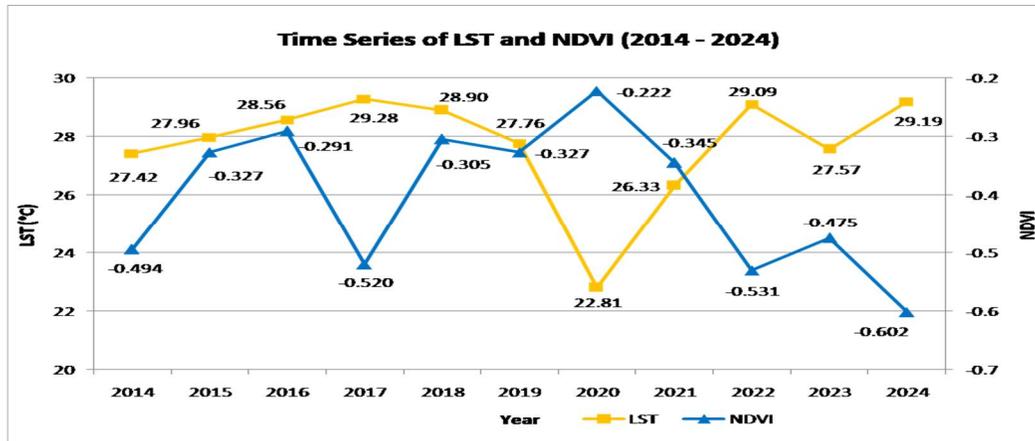
Figure 4. Temporal Analysis of LST and NDVI (2014–2024)

The NDVI values throughout the period between 2014 and 2024 showed a gradual decline, -0.494 in 2014 and -0.602 in 2024 recorded which corresponds to a negative 21.71% change despite the existence of interannual variations. Specifically, NDVI decreased by -0.520 in 2017, the year in which local surface temperature (LST) recorded its high value of 29.28°C, and -0.531 in 2022, when LST jumped to its highest on record. These findings have consistently demonstrated an inverse relationship between vegetation and urban temperatures. Chakraborty et al. (2022) and Kowe et al. (2021) found that larger, more connected vegetation patches are more effective at mitigating land surface temperature (LST). Mumbai shows a slightly higher increment in LST as compared to other cities, an indication of greater land change. This strong inverse relation between LST and NDVI indicates the importance of urban greening measures in mitigating thermal stress and increasing climate resilience, particularly in rapidly growing urban areas.

C. *Trends analysis in Surface Energy Fluxes (2014–2024)*

Figure 5 contains a spatiotemporal analysis of surface energy balance components-Albedo, Net Radiation (R_n), Soil Heat Flux (G), Sensible Heat Flux (H), Latent Heat Flux (LE), and Evapotranspiration (ET) in the years 2014 and 2024.
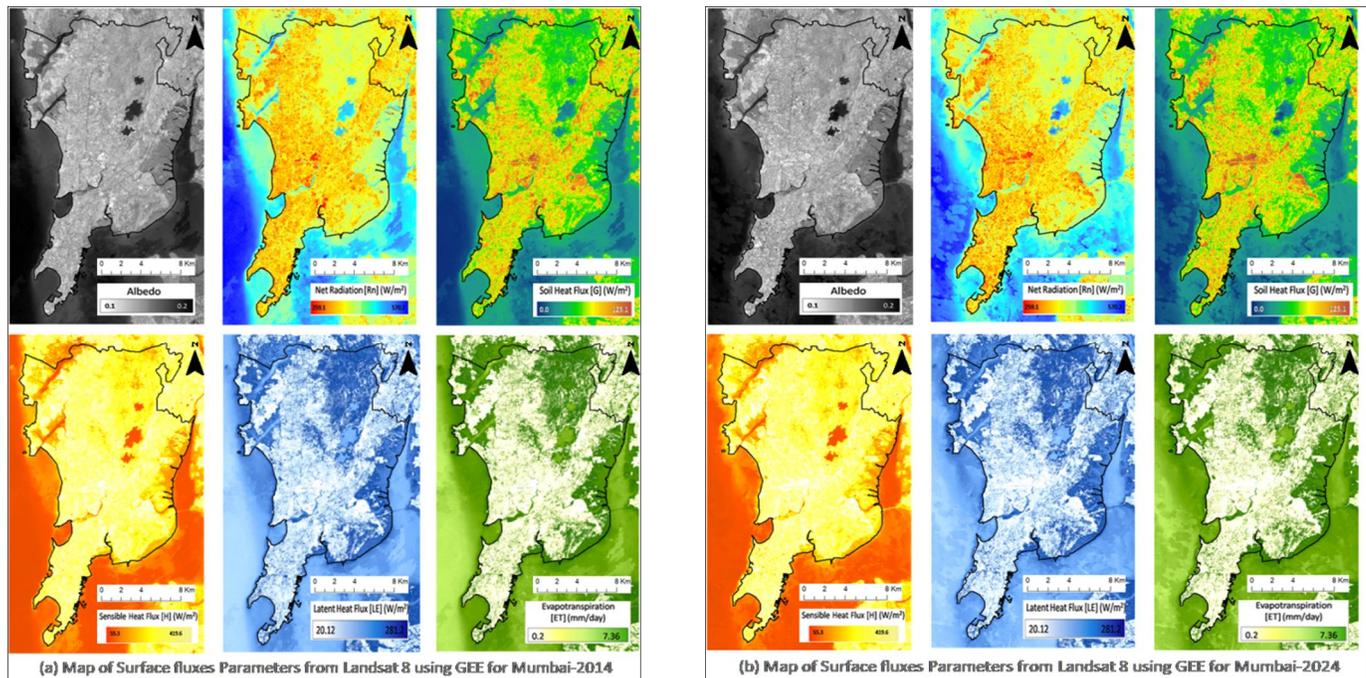

Figure 5. Spatio-temporal Analysis of Surface Fluxes Parameters from Landsat 8 using GEE for Mumbai (a) Year - 2014 (b) Year – 2024

Albedo maps are highly constant with little difference in surface reflectance in the various maps since the decade; however, a substantial difference in the albedo maps of urban areas as the increase in impervious covers leads to reduced albedo readings. The Net radiation has slightly increased in 2024, especially in the urban cores, because of continued urbanization, which is in line with the rising values of the Soil Heat Flux (G) and Sensible Heat Flux (H) rates, indicating that there was greater heating of the surface and urban heat island effects. Conversely, LE and ET maps indicate comparatively constant and marginally greater values, especially across vegetated and peri-urban regions, which could be due to trees-planting activities, and better management of the land. These results are similar to those of earlier researches by Rios et al., (2022) and Smith et al., (2021) that observed urbanized areas with high impervious surface area percentages experience increased sensible heat flux and land surface temperature, while areas with higher vegetation coverage exhibit higher latent heat flux and lower temperatures. This study show that anthropogenic heat discharge contributes to urban warming, with greater impacts in high-density urban areas. Understanding these dynamics is crucial for developing effective urban climate change adaptation strategies.
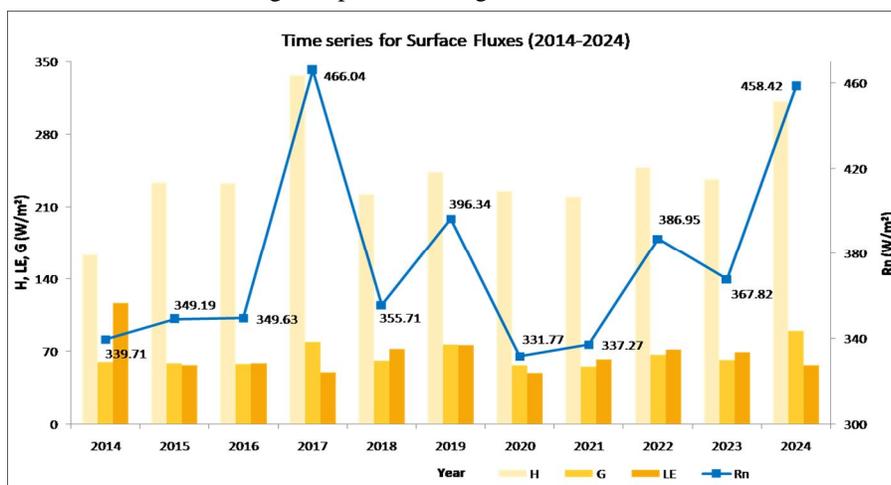

Figure 6. Temporal Analysis of Surface Fluxes (2014–2024)

Decadal analysis of surface energy fluxes in Mumbai between 2014 and 2024 shows (Fig. 6) that there is a major change in urban surface energy balance, which is also closely related to land cover change and an increase in LST. Net radiation (Rn) showed a consistent growth from 339.71 W/m² in 2014 to a high point of 548.42 W/m² by the year 2024, an increase of 34.94%. The growth was significantly higher in 2017 (466.04 W/m²) and 2022 (386.95 W/m²). The sensible heat flux (H) was the determining factor in the proportions of the energy distribution during the timeframe, with averagely steady high values of 250-350 W/m², and it peaked in the year 2017, a time when there was less plant coverage (NDVI: -0.520) and LST was higher (29.28°C). In comparison, latent heat flux (LE) was restrained with an average amount of 50-120 W/m² and an obvious decrease in the years of strong surface warming. Ground heat flux (G) was less variable and tended to be in the range of 50-80 W/m². These findings suggest that the role of sensible heat is increasing gradually, which is associated with the decline in the vegetation cover and evapotranspiration, which is also observed by Wang et al., (2021). Urban and impervious surfaces show higher sensible heat flux ratios, while vegetation and water bodies display higher latent heat flux ratios described by Bala et al., (2022). These findings underscore the importance of strategic urban vegetation planning for effective heat mitigation and climate adaptation in cities.

D. Seasonal Variation in Surface Energy Fluxes (2014–2024)

Analysis of a decade of surface energy flux over Mumbai (2014–2024) provides significant differences in the summer and the monsoon seasons shows in figure (7). The values of net radiation (R_n) are also always higher during summertime, and it approximate values between 400-500 W/m². The higher levels relate to the increased condition of solar isolation and a low extent of cloud cover. Monsoon R_n values vary between 350-400 W/m², These are mostly due to the differences in the solar radiation, the amount of moisture in the atmosphere, and the land-surface properties. The sensible heat flux (H) is also prevailing in summer and is 210-300 W/m 2 and a sharp peak can be observed in 2019. However, monsoon H is more variable, reaching its lowest levels of 150-200 W/m² in wet years like 2016 and 2020.
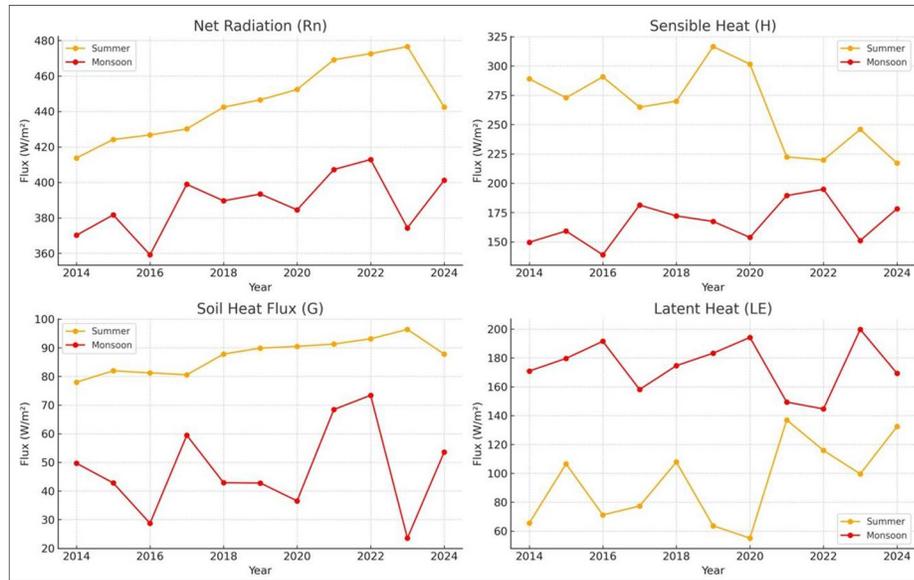
Figure 7. Seasonal variation of Surface Fluxes (2014–2024)

Ground heat flux (G) was slightly larger in summer, with over 100 W/m² during 2023 compared to less than 30 W/m² during the monsoon. The strongest seasonal variation was observed in the latent heat flux (LE), with monsoon LE peaking at more than 190 W/m² throughout 2020 and 2023, whereas LE during summer decreased to less than 60 W/m². These consistently find that urbanized areas have higher sensible heat flux (H) and land surface temperature (LST), while vegetated areas exhibit higher latent heat flux (LE) and lower temperatures (Ren et al., 2022).The innovation of the study is a decade-scale, seasonally resolved evaluation of urban surface energy fluxes based on high-resolution remote sensing data, which allows detection of both the negligibly small interannual variations and even larger long-term signals in urban climates. The correlation analysis with R^2 values of surface fluxes are further elaborated in Section (3.5).

E. Correlation Analysis

In Figure 8, it is exhibited that Net Radiation (R_n) is connected with the surface parameters between 2014 and 2024, such as Land Surface Temperature (LST), Normalized Difference Vegetation Index (NDVI), Albedo, and Evapotranspiration (ET).
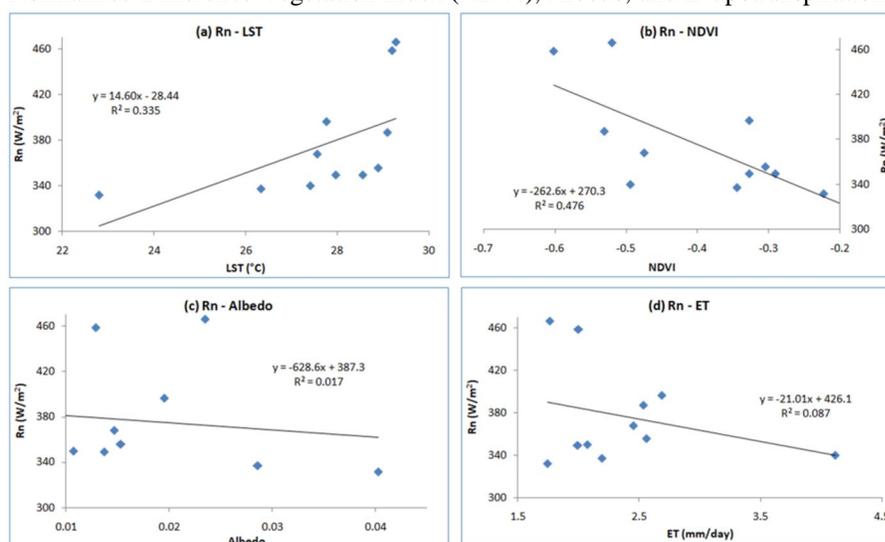

Figure 8. Correlation between (a) Rn – LST, (b) Rn – NDVI, (c) Rn – Albedo, (d) Rn - ET

Rn is the most positively correlated variable with LST (R^2 = 0.335), which is attributed to surface warming caused by urbanization that strongly increases net radiation. The correlation between R_n and NDVI is negative (R^2 = 0.476), indicating the cooling effect of vegetation. These results are specific in that they highlight the moderating effect of vegetation that holds stability through summer and monsoons, even though the urbanization process continues. The net radiation had the greatest and most direct relationship with LST, which is an indication that the level of heating in the urban environment is associated with elevated Radiative forcing (Chen et al., 2024). There is a weak negative correlation of albedo with R_n (R^2 = 0.017) which, observed that albedo has limited influence over dense urban Structures. Correlation between R_n and ET is also weak (R^2 = 0.087), but the negative slope implies the importance of evapotranspiration in decreasing Rn.
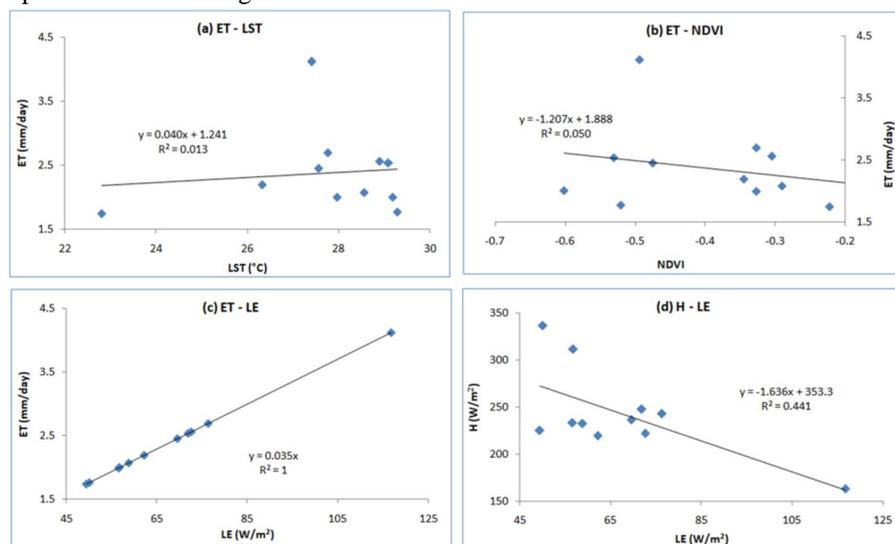

Figure 9. Correlation between (a) ET – LST, (b) ET – NDVI, (c) ET – LE, (d) H – LE

Figure 9 shows the correlation of Evapotranspiration (ET) and the critical surface variables of Land Surface Temperature (LST), Normalized Difference Vegetation Index (NDVI), Latent Heat Flux (LE), and Sensible Heat Flux (H) over the 2014 - 2024 periods in Mumbai, India. The ET and LST relationship depicts strong negative correlation (R^2 = 0.013), indicating that an increase in surface temperatures has a low level effect in reducing ET rates. The correlation between ET and NDVI is positive (R^2 = 0.050), also theoretically, greater vegetation cover should encourage higher ET. In comparison, ET is highly positively correlated with Latent Heat Flux (LE) (R^2 = 1) and highly negatively correlated with Sensible Heat Flux (H) (R^2 = 0.441). These findings are consistent with previous models (Lin et al., 2022), which identify ET as the main driver of energy partitioning, where latent heat flux dominates sensible heat flux in vegetated areas. The originality of the research is associated with the decade-long, multi-variable analysis of ET drivers in a fast urbanizing, semi-arid region conducted with high-resolution satellite information. This study highlights the necessity of preserving green infrastructure and adopting sustainable land management practices to regulate surface energy fluxes, enhance climate resilience, and reduce heat stress in cities undergoing rapid urbanization.

IV.   CONCLUSION

The surface energy balance, land cover change, and thermal patterns of the decadal (2014-2024) spatiotemporal analysis show significant anthropogenic influence on the study site due to the rapid pace of urbanization in Mumbai, India. The urban microclimate has been significantly changed by a 11.9% increase (from 18.6% to 30.5%) in a built-up area and a 21.71% decrease in vegetative cover. In correspondence, there was an increase of 2°C realized in Land Surface Temperature (LST) (i.e., 27.41°C to 29.18°C), which translated to a significant urban heat island effect. An improvement in net radiation (Rn) of 34.94% (339.71W/m² to 458.42W/m²) occurred as a result of decreasing albedo and an increase in impervious surfaces. The most significant energetic factor that dominated was sensible heat flux (H), which still amounted to more than 220 W/m², especially in the years with a decreased vegetation cover and an increase in surface temperatures, like 2017. Conversely, latent heat flux (LE) and evapotranspiration (ET) were subject to less variability and consistently lower values (LE: ~50–100 W/m2), particularly in the summer, due to the cooling effect of urban expansion being counteracted by evaporation. There was a significant positive relationship between the Rn and the LST (R^2 = 0.335) and between LE and ET (R^2 = 1), while H had an inversely proportional

relationship with LE (R² = 0.441), which indicates the moderating effects of vegetation in surface energy partitioning. The results confirm that reduction in vegetative cover, increase in imperviousness, and altered surface flux dynamics are of primary concern in compensating for urban thermal stress. Thus, there is a need to strategically increase green infrastructure and urban climate resilient planning to replenish the surface energy budget and enhance urban resiliency in semi-arid environments. Future studies should extend this research by confirming the findings through ground-based observations at particular sites and by applying this remote sensing-based SEBAL methodology to other cities with comparable semi-arid climates and urban development challenges.

REFERENCES

[1] Sultana, S., & Satyanarayana, A. N. V. (2023). Impact of land use land cover on variation of urban heat island characteristics and surface energy fluxes using WRF and urban canopy model over metropolitan cities of India. Theoretical and Applied Climatology, 152, 97–121. https://doi.org/10.1007/s00704-023-04362-y

[2] Bala, R., Yadav, V. P., Kumar, D. N., & Prasad, R. (2024). Assessment of surface energy fluxes relation with land cover parameters in four distinct Indian cities using remote sensing data. Theoretical and Applied Climatology, 155, 3187–3201. https://doi.org/10.1007/s00704-023-04791-9

[3] Sultana, S., & Satyanarayana, A. N. V. (2021). Impact of urbanization on surface energy balance components over metropolitan cities of India during 2000–2018 winter seasons. Research Square [Preprint]. https://doi.org/10.21203/rs.3.rs-709565/v1

[4] Saxena, D., Choudhary, M., & Sharma, G. (2024). Spatiotemporal trends and evapotranspiration estimation using an improvised SEBAL convergence method for the semi-arid region of Western Rajasthan, India. AQUA, 73(3), 407–423. https://doi.org/10.2166/aqua.2024.220

[5] Rahman, M. M., & Zhang, W. (2019). Review on estimation methods of the Earth's surface energy balance components from ground and satellite measurements. Journal of Earth System Science, 128, 84. https://doi.org/10.1007/s12040-019-1098-5

[6] Eswar, R., Sekhar, M., & Bhattacharya, B. K. (2017). Comparison of three remote sensing based models for the estimation of latent heat flux over India. Hydrological Sciences Journal, 62(16), 2705–2719. https://doi.org/10.1080/02626667.2017.1404067

[7] Zawadzka, J., Corstanje, R., Harris, J. A., & Truckell, I. (2019). Downscaling Landsat-8 land surface temperature maps in diverse urban landscapes using multivariate adaptive regression splines and very high resolution auxiliary data. International Journal of Digital Earth, 12(7), 737–756. https://doi.org/10.1080/17538947.2019.1593527

[8] Firozjaei, M. K., Mijani, N., Kiavarz, M., Duan, S. B., Atkinson, P. M., & Alavipanah, S. K. (2024). A novel surface energy balance-based approach to land surface temperature downscaling. Remote Sensing of Environment, 301, 114087. https://doi.org/10.1016/j.rse.2024.114087

[9] Liang, J., Xie, Y., Sha, Z., & Zhou, A. (2020). Modeling urban growth sustainability in the cloud by augmenting Google Earth Engine (GEE). Computers, Environment and Urban Systems, 84, 101542. https://doi.org/10.1016/j.compenvurbsys.2020.101542

[10] Barletta, C., Capolupo, A., & Tarantino, E. (2022). Exploring the potentialities of Landsat 8 and Sentinel-2 satellite data for estimating the land surface albedo in urban areas using GEE platform. In Communication Systems and Applications (pp. 369–377). Springer. https://doi.org/10.1007/978-3-031-10545-6_30

[11] Taheri, M., Mohammadian, A., Ganji, F., Bigdeli, M., & Nasseri, M. (2022). Energy-based approaches in estimating actual evapotranspiration focusing on land surface temperature: A review of methods, concepts, and challenges. Energies, 15(4), 1264. https://doi.org/10.3390/en15041264

[12] Ramírez-Cuesta, J., Consoli, S., Longo, D., Longo-Minnolo, G., Intrigliolo, D., & Vanella, D. (2024). Influence of short-term surface temperature dynamics on tree orchards energy balance fluxes. Precision Agriculture, 24, 284–303. https://doi.org/10.1007/s11119-022-09891-6

[13] Bala, R., Yadav, V., Kumar, D., & Prasad, R. (2022). Assessment of surface energy fluxes variation with land cover parameters using Landsat satellite data. In 2022 URSI Regional Conference on Radio Science (URSI-RCRS) (pp. 1–4). IEEE. https://doi.org/10.23919/URSI-RCRS56822.2022.10118439

[14] Anand, N., Satheesh, S., & Moorthy, K. K. (2022). Land–atmosphere interactions at a semi-arid region in the Deccan Plateau. Journal of Geophysical Research: Atmospheres, 127(24), e2022JD037211. https://doi.org/10.1029/2022JD037211

[15] Wetherley, E. B., Roberts, D., Tague, C., Jones, C., Quattrochi, D., & McFadden, J. (2021). Remote sensing and energy balance modeling of urban climate variability across a semi-arid megacity. Urban Climate, 35, 100757. https://doi.org/10.1016/j.uclim.2020.100757

[16] Estoque, R. C., Murayama, Y., & Myint, S. W. (2017). Effects of landscape composition and pattern on land surface temperature: An urban heat island study in the megacities of Southeast Asia. Science of the Total Environment, 577, 349–359. https://doi.org/10.1016/j.scitotenv.2016.10.195

[17] Rahaman S, Jahangir S, Haque MS, Chen R, Kumar P. Spatio-temporal changes of green spaces and their impact on urban environment of Mumbai, India. Environment, Development and Sustainability. 2021;23(9):13655-13677. https://doi.org/10.1007/s10668-020-00882-z

[18] Sharma, S., Nahid, S., Sannigrahi, S., Zhang, Q., Basu, B., Ghosh, S., Chakraborti, S., Sen, S., & Joshi, P. K. (2020). A long-term and comprehensive assessment of urbanization-induced impacts on ecosystem services in the capital city of India. City and Environment Interactions, 7, 100047. https://doi.org/10.1016/j.cacint.2020.100047

[19] Naikoo, M. W., Rihan, M., Shahfahad, M., Ahmed, R., Rahman, A., Kafy, A.-A., Rahman, M. A., & Ullah, K. (2023). Analysis of peri-urban land use/land cover change and its drivers using geospatial techniques and geographically weighted regression. Environmental Science and Pollution Research, 30(55), 116973–116989. https://doi.org/10.1007/s11356-022-18853-4

[20] Muhaimin, M., Arisanty, D., Adyatma, S., Saputra, A. N., & Jumriani, J. (2024). Utilization of Landsat 8 OLI TIRS for environmental quality spatial modeling. IOP Conference Series: Earth and Environmental Science, 1421(1), 012010. https://doi.org/10.1088/1755-1315/1421/1/012010

[21] United States Geological Survey. (2024). Landsat 8 (L8) data users handbook. https://www.usgs.gov/landsat-missions/landsat-8-data-users-handbook

[22] Govil, H., Guha, S., Diwan, P., Gill, N., & Dey, A. (2019). Analyzing linear relationships of LST with NDVI and MNDISI using various resolution levels of Landsat 8 OLI and TIRS data. In P. K. Pattnaik, S. Dehuri, B. B. Sahoo, & S. C. Satapathy (Eds.), Data management, analytics and innovation (pp. 139–149). Springer. https://doi.org/10.1007/978-981-32-9949-8_13

[23] Ermida, S. L., Soares, P., Mantas, V., Göttsche, F. M., & Trigo, I. F. (2020). Google Earth Engine open-source code for land surface temperature estimation from the Landsat series. Remote Sensing, 12(9), 1471. https://doi.org/10.3390/rs12091471

[24] Nikkala, S., Peddada, J. R., & Neredimelli, R. (2022). Correlation analysis of land surface temperature on Landsat-8 data of Visakhapatnam urban area, Andhra Pradesh, India. Earth Science Informatics, 15, 1963–1975. https://doi.org/10.1007/s12145-022-00850-3

[25] Shirani-Bidabadi, N., Nasrabadi, T., Faryadi, S., Larijani, A., & Shadman Roodposhti, M. (2019). Evaluating the spatial distribution and the intensity of urban heat island using remote sensing, case study of Isfahan city in Iran. Sustainable Cities and Society, 45, 686–692. https://doi.org/10.1016/j.scs.2018.12.005

[26] Dissanayake, D. M. S. L. B., Morimoto, T., Ranagalage, M., & Murayama, Y. (2019). Land-use/land-cover changes and their impact on surface urban heat islands: Case study of Kandy City, Sri Lanka. Climate, 7(8), 99. https://doi.org/10.3390/cli7080099

[27] Simwanda, M., Ranagalage, M., Estoque, R. C., & Murayama, Y. (2019). Spatial analysis of surface urban heat islands in four rapidly growing African cities. Remote Sensing, 11(14), 1645. https://doi.org/10.3390/rs11141645

[28] Sultana, S., & Satyanarayana, A. N. V. (2020). Assessment of urbanisation and urban heat island intensities using Landsat imageries during 2000–2018 over a sub-tropical Indian city. Sustainable Cities and Society, 52, 101846. https://doi.org/10.1016/j.scs.2019.101846

[29] Patel, M., Desai, D., & Shah, Z. (2025). Satellite-based trends analysis of land surface temperature, vegetation growth, and precipitation: Evaluating seasonal variation and correlation in Ahmedabad, India. Indian Journal of Science and Technology, 18(20), 1538–1546. https://doi.org/10.17485/IJST/v18i20.638

[30] Barletta, C., Capolupo, A., & Tarantino, E. (2022). Exploring the potentialities of Landsat 8 and Sentinel-2 satellite data for estimating the land surface albedo in urban areas using GEE platform. In Communication Systems and Applications (pp. 369–377). Springer. https://doi.org/10.1007/978-3-031-10545-6_30

[31] Ferreira, T., Silva, B. B., Moura, M. S. B., Verhoef, A., & Nóbrega, R. L. B. (2020). The use of remote sensing for reliable estimation of net radiation and its components: A case study for contrasting land covers in an agricultural hotspot of the Brazilian semiarid region. Agricultural and Forest Meteorology, 291, 108052. https://doi.org/10.1016/j.agrformet.2020.108052

[32] Silva, B. B., Mercante, E., Vilas Boas, M. A., Wrublack, S. C., & Oldoni, L. V. (2018). Satellite-based ET estimation using Landsat 8 images and SEBAL model. Revista Ciência Agronômica, 49(2), 221–227. https://doi.org/10.5935/1806-6690.20180025

[33] Desai, D., Mallick, K., Bhattacharya, B. K., Bhat, G. S., Morrison, R., Cleverly, J., et al. (2022). A coupled ground heat flux–surface energy balance model of evaporation using thermal remote sensing observations. Biogeosciences Discussions, 1–45. https://doi.org/10.5194/bg-2021-356

[34] Liang, A., Xie, C., Wang, J., & Che, S. (2022). Daily dynamics of soil heat flux and its relationship with net radiation in different urban riparian woodlands. Forests, 13(12), 2062. https://doi.org/10.3390/f13122062

[35] Rios, G., & Ramamurthy, P. (2022). A novel model to estimate sensible heat fluxes in urban areas using satellite-derived data. Remote Sensing of Environment, 280, 112880. https://doi.org/10.1016/j.rse.2021.112880

[36] Jaiswal, N., Deb, S., & Kishtawal, C. (2023). Development of a hybrid model to predict air temperature over an urban area: A case study over Ahmedabad, India. Atmospheric Research, 292, 106876. https://doi.org/10.1016/j.atmosres.2023.106876

[37] Patel, A., Vyas, D., Chaudhari, N., Patel, R., Patel, K., & Mehta, D. (2024). Novel approach for the LULC change detection using GIS & Google Earth Engine through spatiotemporal analysis to evaluate the urbanization growth of Ahmedabad city. Results in Engineering, 21, 101788. https://doi.org/10.1016/j.rineng.2024.101788

[38] Mohammad, P., Goswami, A., & Bonafoni, S. (2019). The impact of the land cover dynamics on surface urban heat island variations in semi-arid cities: A case study in Ahmedabad city, India, using multi-sensor/source data. Sensors, 19(17), 3701. https://doi.org/10.3390/s19173701

[39] Rawal, D., & Gupta, V. K. (2021). UHI spatio-temporal analysis with geospatial techniques: A case of Ahmedabad city. Paripex - Indian Journal of Research, 10(9), 10–14. https://doi.org/10.36106/paripex/1912691

[40] Mathew, A., P. S., & Khandelwal, S. (2022). Investigating the contrast diurnal relationship of land surface temperatures with various surface parameters representing vegetation, soil, water, and urbanization over Ahmedabad city in India. Energy Nexus, 7, 100044. https://doi.org/10.1016/j.nexus.2022.100044

[41] Agarwal, S., Rao, P., & Nagendra, H. (2023). Fifteen years of fragmentation and land cover change in India's ten largest cities – A Google Earth Engine analysis. Cities and the Environment, 16(2), Article 2. https://doi.org/10.15365/cate.2023.160202

[42] Vaishnav, K., Kanga, S., Sajan, B., Singh, S., Singh, S., Debnath, J., et al. (2024). Assessment of Dyna-CLUE model for prediction of spatio-temporal dynamics of urbanisation and green space in Jaipur district, Rajasthan (India). Discover Cities, 4, 100023. https://doi.org/10.1007/s44327-024-00023-5

[43] Agan, P. (2021). Urban heat island effects; A de-greening process, implication for environmental sustainability and quality of urban life: A review. Advances in Hydrology and Meteorology, 1(1), 1–5. https://doi.org/10.33552/ahm.2021.01.000505

[44] Chakraborty, T., Venter, Z., Qian, Y., & Lee, X. (2022). Lower urban humidity moderates outdoor heat stress. AGU Advances, 3, e2022AV000729. https://doi.org/10.1029/2022AV000729

[45] Kowe, P., Mutanga, O., Odindi, J., & Dube, T. (2021). Effect of landscape pattern and spatial configuration of vegetation patches on urban warming and cooling in Harare metropolitan city, Zimbabwe. GIScience & Remote Sensing, 58(1), 108–125. https://doi.org/10.1080/15481603.2021.1877008

[46] Smith, I., Winbourne, J. B., Tieskens, K., Jones, T., Bromley, F. L., Li, D., et al. (2021). A satellite-based model for estimating latent heat flux from urban vegetation. Frontiers in Ecology and Evolution, 9, 695995. https://doi.org/10.3389/fevo.2021.695995

[47] Wang, R., Li, L., Gentine, P., Zhang, Y., Chen, J., Chen, X., et al. (2021). Recent increase in the observation-derived land evapotranspiration due to global warming. Environmental Research Letters, 16(12), 124059. https://doi.org/10.1088/1748-9326/ac4291

[48] Ren, X., Zhang, Q., Yue, P., Yan, X., & Yang, Y. (2022). Energy distribution characteristics and environmental impact factors in different regions of the summer monsoon transition zone. Frontiers in Environmental Science, 10, 847725. https://doi.org/10.3389/fenvs.2022.847725

[49] Chen, L., Chen, H., Du, X., & Wang, R. (2024). Retrieval of surface energy fluxes considering vegetation changes and aerosol effects. Remote Sensing, 16(4), 668. https://doi.org/10.3390/rs16040668

[50] Lin, H., Li, Y., & Zhao, L. (2022). Partitioning of sensible and latent heat fluxes in different vegetation types and their spatiotemporal variations based on 203 FLUXNET sites. Journal of Geophysical Research: Atmospheres, 127(20), e2022JD037142. https://doi.org/10.1029/2022JD037142
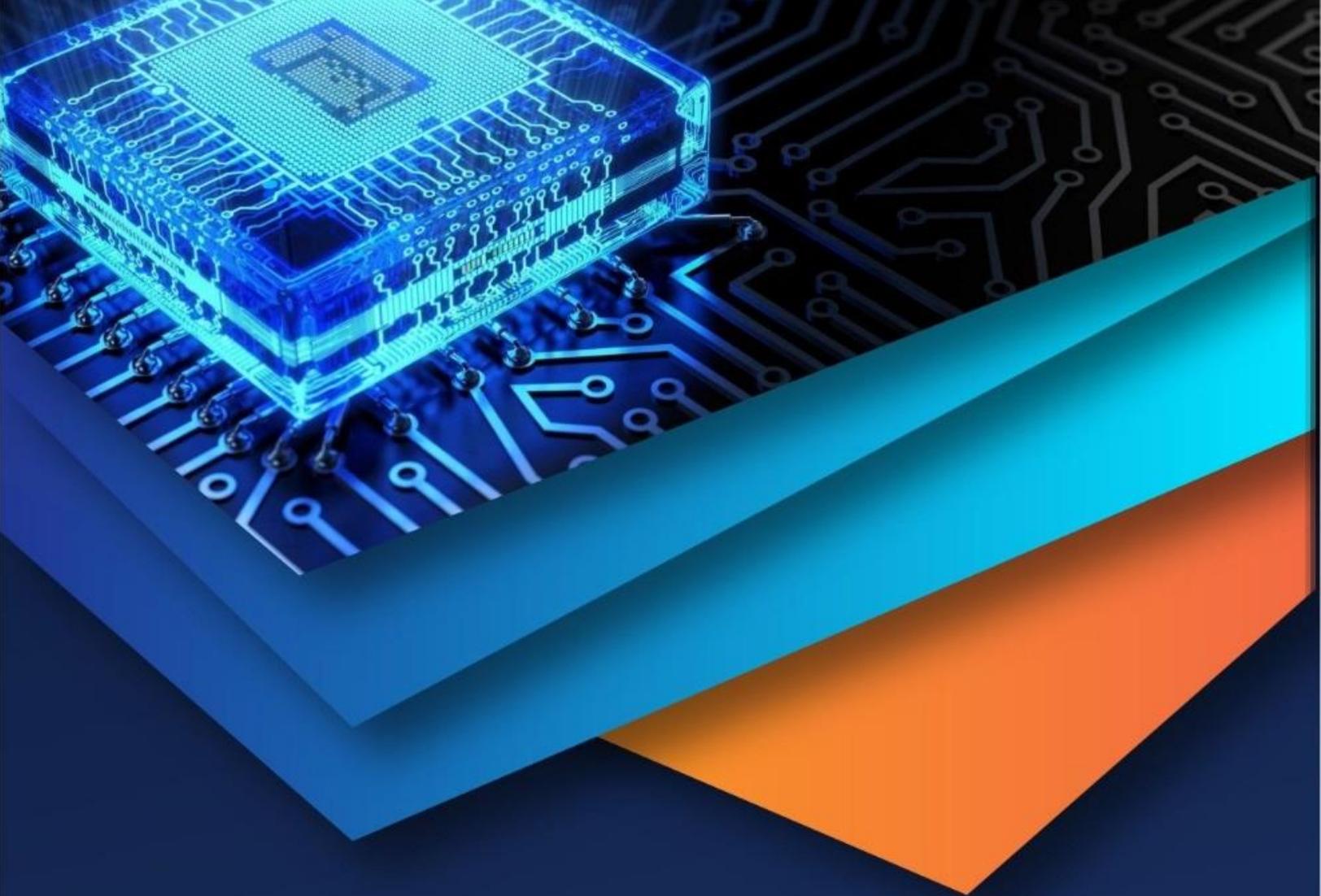
INTERNATIONAL JOURNAL
FOR RESEARCH

IN APPLIED SCIENCE & ENGINEERING TECHNOLOGY

Call : 08813907089 ⊙ (24*7 Support on Whatsapp)